Supporting Information

Ligand Engineering of Au_{44} Nanoclusters for NIR-II Luminescent and Photoacoustic Imaging-Guided Cancer Photothermal Therapy

Ge Yang,[a] Xueluer Mu,[b] Xinxin Pan,[a] Ying Tang,[b] Qiaofeng Yao,[c] Yaru Wang,[a] Fuyi Jiang,[d] Fanglin Du,[a] Jianping Xie,[c,e] Xianfeng Zhou,*[b] and Xun Yuan*[a]*

Table of Contents

Part I. Materials and instrumentation

All materials were used as received without further purification. Ultrapure Millipore water was used throughout the study. All glassware and magnetic stir bars were washed with aqua regia, rinsed with ethanol and water, and then dried in an oven at 90 °C before use. Hydrogen tetrachloroaurate (III) hydrate ($HAuCl_4 \cdot 3H_2O$), 1-(3-dimethylaminopropyl)-3-ethylcarbodiimide hydrochloride (EDC, ≥ 98 %) and N-hydroxysuccinimide (NHS, ≥ 98 %) were purchased from Sigma-Aldrich. Sodium hydroxide (NaOH, ≥ 96 %), sodium chloride (NaCl), ethanol (C_2H_5OH, ≥ 99.0 %), N, N-dimethylformamide (DMF, ≥ 96 %) were purchased from Sinopharm Chemical Reagent Co., Ltd. Tetrahydroborate ($NaBH_4$, ≥ 96 %) was purchased from Shanghai Shanpu Chemical Co., Ltd (China). 4-mercaptobenzoic acid (*p*-MBA) was purchased from TCI. Hoechst 33342, MitoTracker Green, LysoTracker Green, Calcein (AM) & ethidium homodimer-1 (EthD-1) were ordered from Invitrogen (Carlsbad, CA). Other chemicals and solvents were purchased from Energy Chemical Reagent.

UV-vis absorption spectra were obtained on a Shimadzu UV-1800 photospectrometer. Photoluminescence (PL) spectra were recorded on a FLS 1000 spectrometer. Dynamic light scattering (DLS) measurement were performed using a NanoBrook Omni from Brookhaven Instruments. The size and structure of samples were studied by transmission electron microscope (TEM, JEM-2100 Plus Electron Microscope) at a 200 kV accelerating voltage. The molecular formula of Au nanoclusters (NCs) was analyzed by a Bruker Impact II ESI-MS system operating in negative ion mode. The electrochemical characterizations were conducted using a CHI761E electrochemical workstation (CH Instruments Ins). The potential sweep cyclic voltammetry (CV) was conducted in 0.1 mol L^{-1} tetrabutylammonium perchlorate (prepared with acetonitrile) via a three-electrode system (reference electrode: Ag/AgCl electrode; counter electrode: platinum foil). Native polyacrylamide gel electrophoresis (PAGE) was carried out

on an electrophoresis cell system (Mini-PROTEAN Tetra Cell, Bio-Rad Laboratories, Inc). 30 wt% and 4 wt% of acrylamide monomers were prepared for resolving and stacking gels, respectively. Sample solutions were loaded in stacking gel. The electrophoresis is allowed to run at 4 °C for 4 h with a constant voltage of 170 V. The Fourier transform infrared (FTIR) spectra were acquired on a Nicolet iS10 spectrometer. The content of the Au species was determined by inductively coupled plasma mass spectrometry (ICP-MS, Agilent 720-ES). PL images of cells were taken with a laser scanning confocal microscope (Nikon C2+). Live/Dead stained cell images were obtained on an OLYMPUS IX73 inverted microscope. In vivo photoacoustic (PA) imaging was conducted at different time intervals using a LOIS-3D imaging system (TomoWave) with 750 nm laser, and NIR-II PL imaging was conducted using a NIR-II PL in vivo imaging system (Series III 900/1700) with 808 nm laser. H&E-stained images were taken by an OLYMPUS IX73 inverted microscope.

Part II. Synthesis of the alkynylated Cy7 molecules (i.e., Cy7-TCF-3)

Compound 1 and **2** were synthesized as previously described.[1]

Synthesis of **compound 3**: According to a reported protocol,[2] sodium hydride (60% in paraffin, 0.72 g, 18.00 mmol) was resolved in 15 mL anhydrous DMF with a 250 mL round-bottom flask and stirred for 30 min. 4-(4 hydroxyphenyl) cyclohexanone (3.42 g, 18 mmol) which was resolved in 15 mL anhydrous DMF was added slowly at 0 °C. Propargyl bromide (1.43 g, 12.00 mmol) in 100 mL anhydrous DMF was dropwisely added into above solution within 60 min. The reacting mixture was stirred overnight at 25 °C, and the reaction was quenched by adding water. After extracted with CH_2Cl_2 for three times, the organic layer was washed with saturated NaCl aqueous, and then dried over by anhydrous Na_2SO_4. After concentrated, the residue was purified by silica column chromatography with CH_2Cl_2 as eluent to give a white solid (2.09 g, yield: 51%). ^{1}H NMR (500 MHz, $CDCl_3$, δ): 7.18 (d, 2H), 6.94 (d, 2H), 4.68 (d, 2H), 3.00 (m, 1H), 2.52 (m, 5H), 2.18 (m, 2H), 1.91 (m, 2H) (Fig. S4).

Compound 4: According to a reported protocol with some modification,[3] 30 mL of $POCl_3$ (32.90 mL, 212.0 mmol) in DCM was added dropwise to a chilled solution of DMF (30.00 mL, 409.50 mmol) in 30 mL CH_2Cl_2 under N_2 atmosphere under an ice bath. After 30 min, compound 3 was added (9.00 g, 40.00 mmol). The resulting mixture was refluxed with vigorous stirring for 3 h at 80 °C, and then poured into ice-cold water. The crude product was kept overnight to obtain compound 4 as a yellow solid without purification. Yield: 86.5%.

Synthesis of **compound 5**: According to a reported protocol,[3] compound 1 (0.72 g, 3.63 mmol) and compound 4 (1.00 g, 3.30 mmol) were dissolved in absolute ethanol (50 mL). The solution was brought to reflux overnight. The red precipitate was filtered and dried under vacuum to afford compound 5 as a deep red solid without purification. Yield: 79.6%.

Synthesis of **compound Cy7-TCF-3**: According to a reported protocol with some modification,[4] to a solution of compound 5 (1.00 g, 1.95 mmol) in 50 ml anhydrous ethanol, compound 2 (0.40 g, 2.15 mmol) was added along with a drop of pyridine. The resulting solution was refluxed overnight. The precipitate was filtered and purified using column chromatography (dichloromethane) to afford Cy7-TCF-3 as a green solid. Yield: 68.8%. ^{1}H NMR (500 MHz, $CDCl_3$, δ): 8.22 (d, 1H), 8.07 (d, 1H), 7.30 (d, 1H), 7.28 (m, 4H), 7.09 (m, 1H), 7.04 (d, 2H), 6.85 (d, 1H), 6.25 (d, 1H), 5.65 (d, 1H), 4.74 (d, 2H), 3.83 (m, 2H), 2.98 (m, 2H), 2.90 (d, 1H), 2.56 (t, 3H), 1.73 (s, 6H), 1.68 (s, 6H), 1.30 (t, 3H).

Part III. Synthesis of $Au_{44}MBA_{26}$ NCs and $Au_{44}MBA_{26}$-Cy7 NCs[5]

Stock solutions of $HAuCl_4$ (20 mM) and *p*-MBA (20 mM) were prepared with ultrapure water and ethanol, respectively. In a typical synthesis of $Au_{44}MBA_{26}$ NCs, aqueous solutions of $HAuCl_4$ (0.25 mL) as Au precursor, *p*-MBA (0.5 mL) as protecting ligand, and NaOH (1 M, 0.5 mL) were mixed in ~35 % of ethanol (1.224 mL of ethanol and 2.176 mL of water) under stirring condition, leading to the formation of MBA-Au(I) complexes. Afterwards, 0.1 mL of $NaBH_4$ solution (~112 mM, prepared by dissolving 43 mg of $NaBH_4$ powder in 10 mL of 0.2

M NaOH solution) was introduced to the solution drop by drop. The MBA-protected Au_{44} NCs were collected after 24 h of reaction for further characterization.

The synthesis of $Au_{44}MBA_{26}$-Cy7 NCs is conducted as follows. At room temperature, 5 mL of $Au_{44}MBA_{26}$ NCs was centrifuged and dried, and then was added in a 20 mL glass bottle containing ~35 % of ethanol (1.75 mL of ethanol and 3.25 mL of water). Subsequently, 6 mg of EDC and 1.8 mg of NHS were separately added to the solution. After stirring for 30 min, 95.8 μL of the small molecule containing an azide group (20 mM, prepared with ultrapure water) was introduced to the solution, followed by stirring for 2 h to obtain $Au_{44}MBA_{26}$-N_3 NCs. Later on, 1.9 mL of $Au_{44}MBA_{26}$-N_3 NCs was centrifuged and dried, and then was added in a 20 mL glass bottle wrapped in aluminum foil containing 1.854 mL DMF. Afterwards, 146 μL of Cy7 molecules (5 mM, dissolved in DMF) and 7.28 μL of Cu(I) catalyst were separately introduced into the reaction system, followed by stirring in ice water bath for 16 h. After returning to room temperature, the reaction solution was washed with 8 mL water and then centrifuged for 10 min at 12000 rpm to obtain $Au_{44}MBA_{26}$-Cy7 NCs. The preparation of Cu(I) catalyst is as follows: Stock solutions of $CuSO_4$ (50 mM) and *p*-MBA (50 mM) were prepared with ultrapure water and ethanol, respectively. Aqueous solutions of $CuSO_4$ (0.2 mL), *p*-MBA (0.4 mL) and NaOH (1 M, 0.2 mL) were mixed in ~35% of ethanol (1.35 mL of ethanol and 2.85 mL of water) under stirring condition. After stirring of 10 min, the Cu(I)-MBA complexes were collected as the catalyst of click chemistry.

Part IV. Cell culture and imaging

HeLa cells (American Type Culture Collection, ATCC, Manassas, VA) were cultured in DMEM) containing 10 % FBS (fetal bovine serum) and 1 % P/S (penicillin/streptomycin) at 37 °C in an atmosphere of 5 % CO_2 and 95% air. For in vitro PL imaging, these cells were seeded on a 24-well plate at 2×10^4 cells per well for 2 d in 1 mL medium to reach 50-70 % confluency. Certain amount of Hoechst 33342 and $Au_{44}MBA_{26}$-Cy7 NCs were added to the medium to

make their final concentrations to be 5 μM and 0.5 μM, respectively. After 30 min of incubation, cells were washed with PBS several times. The PL images were taken on a confocal fluorescence microscope (Nikon C2+) at the excited wavelengths of 405 nm and 640 nm.

Part V. NIR-II PL and PA imaging in vivo

All animal experiments were approved by the Department of Science and Technology of Shandong Province and the Laboratory Animal Center of Qingdao Zhong Hao Biological Engineering Co., Ltd. To establish tumor-bearing mouse model, approximately 2.5×10^6 4T1 cells in 35 μL PBS buffer were mixed with matrigel (BD, BioCoat, USA) in 1:1 ratio and subcutaneously injected in the right of female BALB/c nude mice (6 six weeks old, ~ 15 g). After 5 d of tumor formation, $Au_{44}MBA_{26}$-Cy7 NCs (500 μM, 200 μL) dispersed in saline were intravenously injected into mice. After injection, PAI and videos were taken for different time using LOIS-3D imaging system (TomoWave) with 750 nm laser. Another batch of female nude mice was injected with 4T1 cells in the right rear claws. After 12 d of tumor formation, $Au_{44}MBA_{26}$-Cy7 NCs (500 μM, 200 μL) dispersed in saline were intravenously injected into mice. After injection, NIR-II imaging was conducted using NIR-II PL in vivo imaging system (Series III 900/1700) with 808 nm laser.

Part VI. In vivo PTT

For in vivo PTT, approximately 2.5×10^6 4T1 cells suspended in 35 μL PBS buffer were mixed with matrigel (BD, BioCoat, USA) in 1:1 ratio and were injected into the right flank of BALB/c nude mice to establish tumor-bearing mouse model. When the average tumor volume reached about 50 mm^3, the mice were randomly divided into 5 groups. The experimental group was named as "$Au_{44}MBA_{26}$-Cy7 + Laser", while the four control groups were named as "Saline", "Saline + Laser", "$Au_{44}MBA_{26}$ + Laser", and "$Au_{44}MBA_{26}$-Cy7". Mice in "Saline" and "Saline + Laser" groups were injected with saline (200 μL) through tail vein, while mice in "$Au_{44}MBA_{26}$ + Laser", "$Au_{44}MBA_{26}$-Cy7" and "$Au_{44}MBA_{26}$-Cy7 + Laser" groups were

injected with $Au_{44}MBA_{26}$ NCs and $Au_{44}MBA_{26}$-Cy7 NCs (500 μM, 200 μL dispersed in saline) through tail vein. The tumor surface of the mice in the Laser groups was irradiated with laser (808 nm, 1 W cm^{-2}) for 10 min, and the IR images of the nude mice were monitored by a thermal imager (FLUKA TiS20). The body weights and tumor volumes of mice were recorded every two d. The body weights were calculated as W/W_0 (W_0: the weight on Day 0, W: the weight recorded during the treatment). Tumor volumes were calculated by the formula:

Tumor volume = length × $(width)^2/2$.

The relative tumor volumes were calculated as V/V_0 (V_0: the volume on Day 0, V: the volume recorded during the treatment). After treatment, the mice were sacrificed and the heart, liver, spleen, lung and kidney were taken out for histology analysis. The tissues were embedded in paraffin cassettes and stained with H&E after dehydration. The haematoxylin and eosin (H&E)-stained images are obtained with an OLYMPUS IX73 inverted microscope.

Part VII. Statistical analysis

All experiments were performed at least three times, and the results were expressed as mean ± SD. Statistical calculation of experimental data was performed using the one-way analysis of variance (ANOVA) statistical analysis. The p values less than 0.05 were considered statistically significant. Significant p values are denoted by $*p < 0.05$.

Supplementary Note

Supplementary Note I: The alkynylated Cy7 molecules (i.e., Cy7-TCF-3) were synthesized in our laboratory (Fig. S2), and their molecular structure was confirmed by ^1H nuclear magnetic resonance (NMR) and high-resolution mass spectrometry (Fig. S3-S5).[1,6] After modifying the surface of $Au_{44}MBA_{26}$ NCs by azide groups via EDC/NHS crosslinking, the amide bond peak at 1638 cm^{-1} and the azide bond peak at 2200 cm^{-1} are observed in the FTIR spectrum of azide-containing $Au_{44}MBA_{26}$ NCs (Fig. S6), indicating the successful grafting of azide groups on $Au_{44}MBA_{26}$ NCs. After that, the azide-containing $Au_{44}MBA_{26}$ NCs were conjugated with alkynylated Cy7 molecules via click chemistry. As shown in Fig. S6, the

absence of the azide band at 2200 cm^{-1} and the appearance of the triazole anion marker band at 1147 cm^{-1} in the FTIR spectrum provide supportive evidence on the successful click chemistry reaction between the azide-containing $Au_{44}MBA_{26}$ NCs and alkynylated Cy7 molecules.[7]

Supplementary Note II: It is curious about how many Cy7 molecules could be conjugated on the $Au_{44}MBA_{26}$ NCs, which is also influential to the photothermal and PA properties of the $Au_{44}MBA_{26}$-Cy7 NCs. Therefore, we conducted experiments to clarify this issue. We first tried to acquire the molecular weight of the $Au_{44}MBA_{26}$-Cy7 NCs by using ESI-MS, but failed probably due to the spectral interference by other residual species such as EDC, NHS, and alkynylated Cy7 molecules. Hence, we turned to utilize colorimetric strategy to determine the number of the conjugated Cy7 molecules on the surface of $Au_{44}MBA_{26}$-Cy7 NCs. Firstly, we prepared a series of alkynylated Cy7 solutions with a known gradient of concentrations, and measured their optical absorbance using UV-vis absorption spectroscopy (Fig. S8a), which enabled us to correlate the concentration of alkynylated Cy7 molecules to their optical absorbance. As shown in Fig. S8b, a linear relationship between the concentration and the optical density of the characteristic absorbance at 843 nm is established. Secondly, we measured the optical density of the DMF solution of the as-synthesized $Au_{44}MBA_{26}$-Cy7 at 843 nm, and then subtracted the absorbance of corresponding $Au_{44}MBA_{26}$ solution. On this basis, the concentration of the conjugated Cy7 molecules on the $Au_{44}MBA_{26}$-Cy7 can be determined to be 176.8 μM by using the linear concentration–absorbance relationship established. According to ICP-MS analysis, the concentration of Au^+ species in the $Au_{44}MBA_{26}$-Cy7 solution was calculated to be 592.49 μM, by which the concentration of $Au_{44}MBA_{26}$ NCs was identified to be 13.47 μM because one cluster contains 44 Au atoms. By comparing the concentrations of the conjugated Cy7 molecules and the $Au_{44}MBA_{26}$ NCs in the $Au_{44}MBA_{26}$-Cy7 NCs, the ratio of $Au_{44}MBA_{26}$ NCs to Cy7 molecules in the obtained $Au_{44}MBA_{26}$-Cy7 NCs was found to be 1 : 13, suggesting that thirteen Cy7 molecules were conjugated to each $Au_{44}MBA_{26}$ NC. It should be mentioned that this result about the ratio of the Cy7 molecules in the $Au_{44}MBA_{26}$-Cy7 is

reasonable based on the following two aspects: 1) the molecular structure of the Cy7 is so bulky that the 26 MBA ligands of Au_{44} NCs are unable to accommodate 26 Cy7 molecules due to the large steric hindrance of the Cy7; 2) the conjugation of 13 Cy7 molecules with 13 out of 26 MBA ligands in the $Au_{44}MBA_{26}$ NCs may have minimum influence on the structural symmetry on the $Au_{44}MBA_{26}$-Cy7 NCs when comparing with the cases that conjugating other number of Cy7 molecules with the NCs, which is probably a natural result of thermodynamics.

Fig. S1-Fig. S12

Fig. S1 The native PAGE result (30 % native gel) of the as-synthesized $Au_{44}MBA_{26}$ NCs.

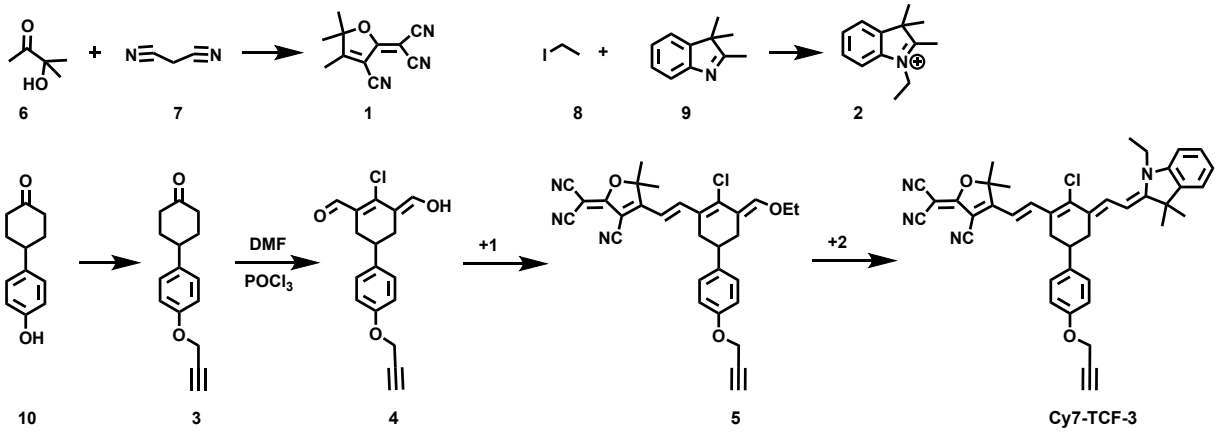

Fig. S2 Synthetic route of the alkynylated Cy7 molecules (i.e., Cy7-TCF-3).

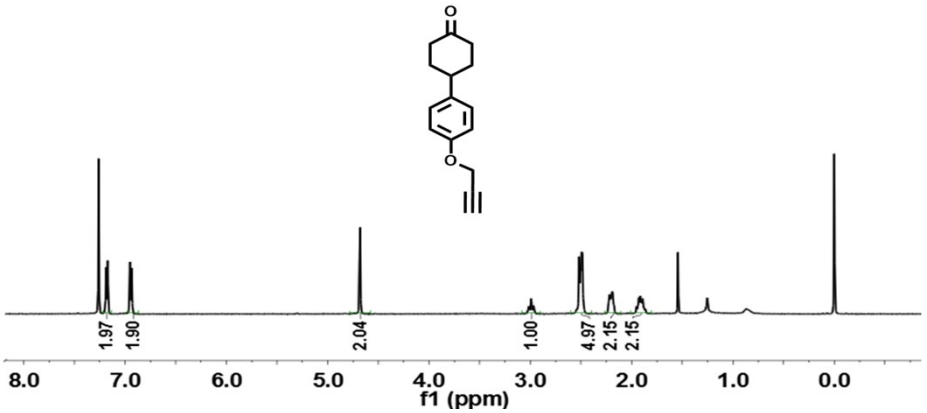

Fig. S3 ^{1}H NMR spectrum of the Compound 3 in $CDCl_3$ at 298 K.

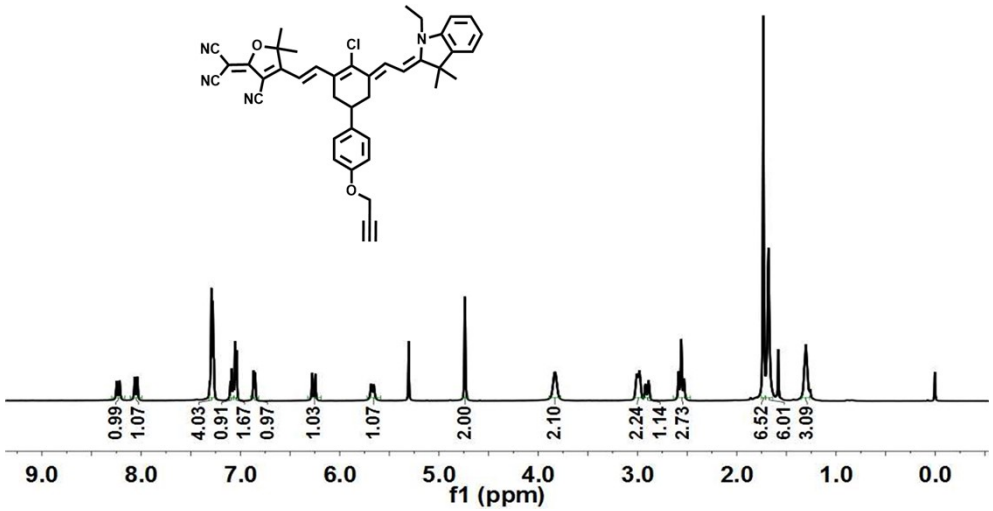

Fig. S4 ^{1}H NMR spectrum of the alkynylated Cy7 molecules (i.e., Cy7-TCF-3) in $CDCl_3$ at 298 K.

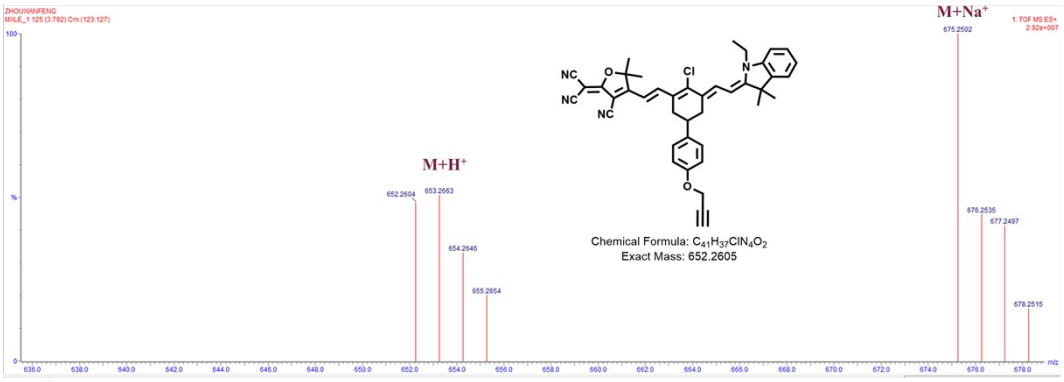

Fig. S5 Mass spectrum of the alkynylated Cy7 molecules (i.e., Cy7-TCF-3) at 298 K.

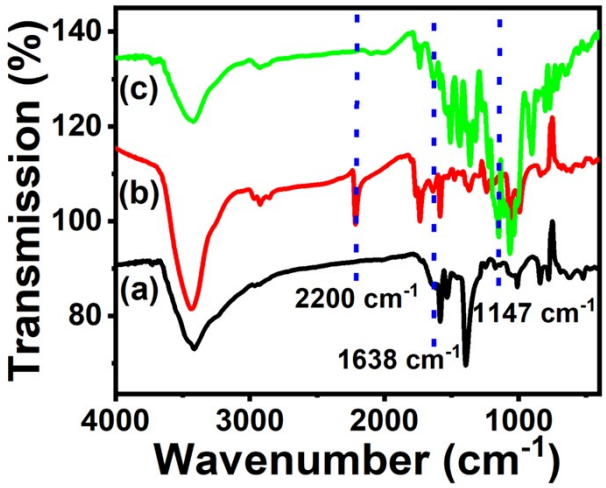

Fig. S6 FTIR spectra of Au_{44} NCs. FTIR spectra of (a) the pristine $Au_{44}MBA_{26}$ NCs, (b) azide-modified $Au_{44}MBA_{26}$ NCs (i.e., $Au_{44}MBA_{26}$-N_3), and (c) as-synthesized $Au_{44}MBA_{26}$-Cy7 NCs.

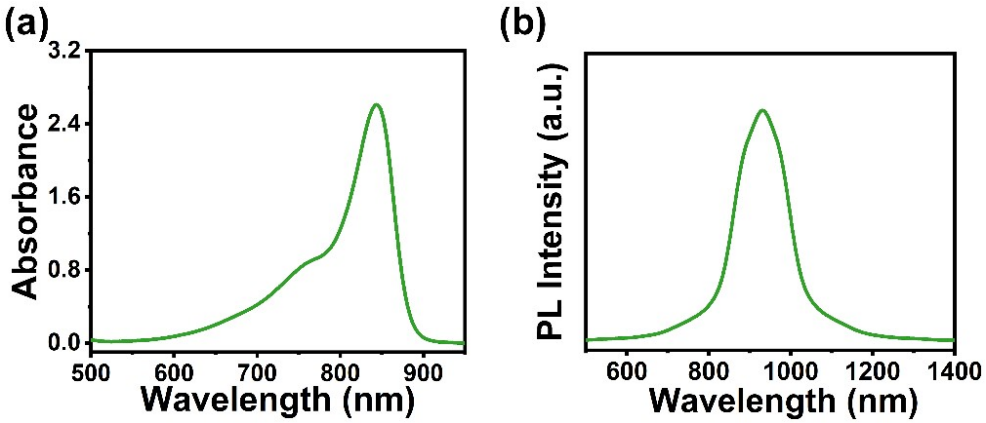

Fig. S7 Properties of Cy7 molecules. (a) UV-vis absorption and (b) PL spectra of alkynylated Cy7 molecules in DMF.

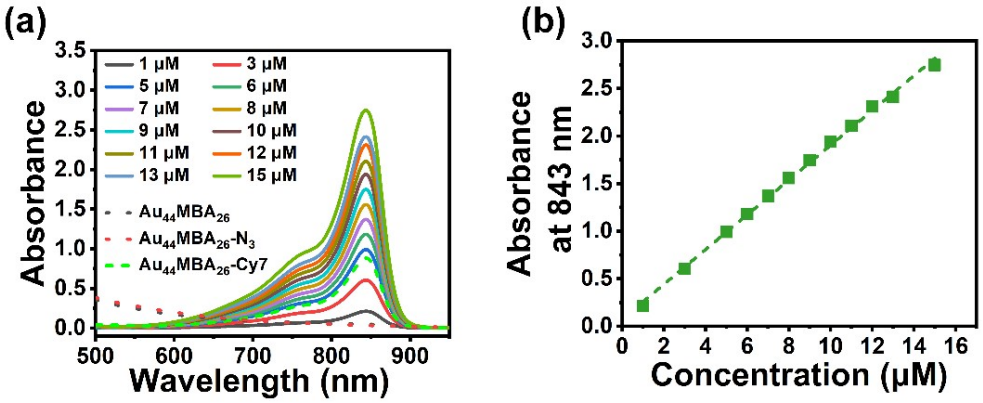

Fig. S8 UV-vis absorption spectra. (a) UV-vis absorption spectra of solutions of alkynylated Cy7 molecules with different concentrations in DMF, pristine $Au_{44}MBA_{26}$ NCs, azide-modified $Au_{44}MBA_{26}$ NCs (i.e., $Au_{44}MBA_{26}$-N_3), and the as-synthesized $Au_{44}MBA_{26}$-Cy7 NCs in DMF. (b) The absorbance at 843 nm of alkynylated Cy7 molecules as a function of their concentration.

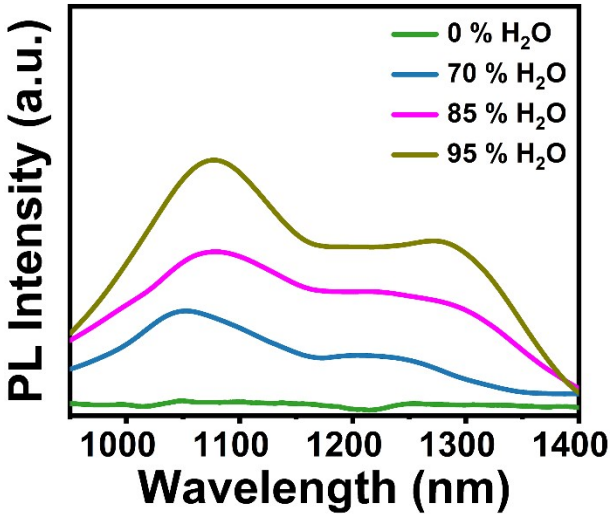

Fig. S9 NIR-II PL emission spectra ($\lambda_{excitation}$ = 808 nm) of $Au_{44}MBA_{26}$-Cy7 NCs in mixed DMF/H_2O solvents.

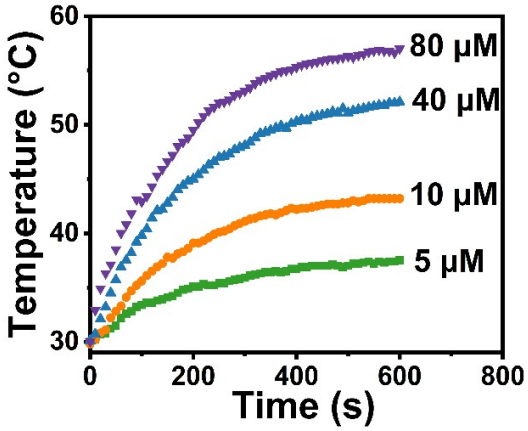

Fig. S10 Time-course temperature elevation profile of aqueous solution of $Au_{44}MBA_{26}$ NCs with different concentrations under laser irradiation (808 nm, 1.5 W cm^{-2}).

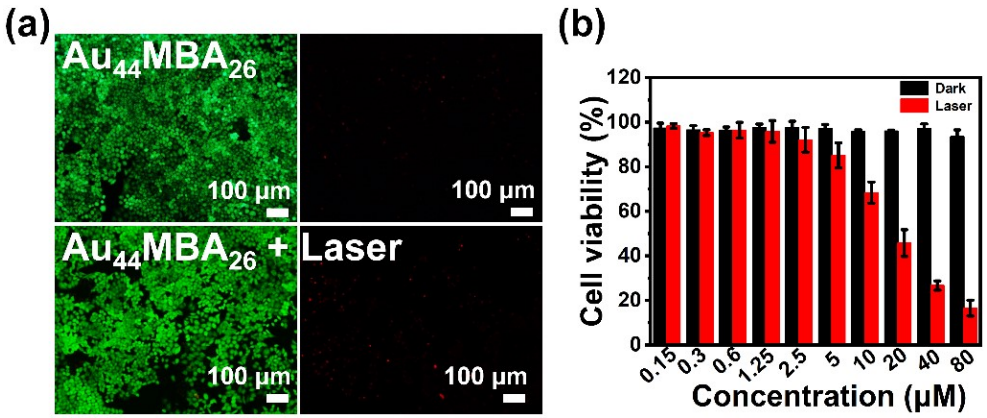

Fig. S11 In vitro PTT of $Au_{44}MBA_{26}$ NCs. (a) PL images of stained HeLa cells treated with 5 μM $Au_{44}MBA_{26}$ NCs without (upper panel) or with (lower panel) 808 nm laser irradiation for 6 min. (b) MTT assay of HeLa cells treated with various concentrations of $Au_{44}MBA_{26}$ NCs (0.15 - 80 μM) with or without laser irradiation.

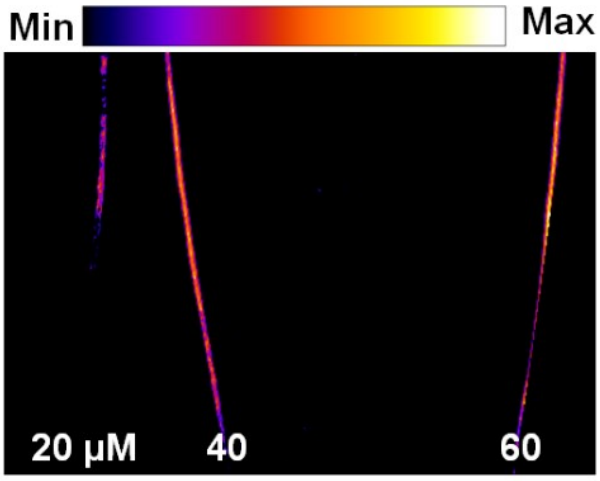

Fig. S12 PA images of pristine $Au_{44}MBA_{26}$ NCs with different concentrations under laser irradiation.

References

1 X. Mu, Y. Lu, F. Wu, Y. Wei, H. Ma, Y. Zhao, J. Sun, S. Liu, X. Zhou and Z. Li, *Adv. Mater.* 2020, **32**, 1906711.

2 X. Han, F. Yu, X. Song and L. Chen, *Chem. Sci.* 2016, **7**, 5098.

3 I. Davydenko, S. Barlow, R. Sharma, S. Benis, J. Simon, T. G. Allen, M. W. Cooper, V. Khrustalev, E. V. Jucov and R. Castañeda, *J. Am. Chem. Soc.* 2016, **138**, 10112.

4 W. Bentoumi, J. C. Mulatier, P. A. Bouit, O. Maury, A. Barsella, J. P. Vola, E. Chastaing, L. Divay, F. Soyer, P. Le Barny, Y. Bretonniere and C. Andraud, *Chem. Eur. J.* 2014, **20**, 8909.

5 X. Zhang, Z. Wang, S. Qian, N. Liu, L. Sui and X. Yuan, *Nanoscale* 2020, **12**, 6449.

6 X. Mu, Y. Tang, F. Wu, H. Ma, S. Huang, M. Liang, J. Yang, Y. Lu, X. Zhou and Z. Li, *ACS Appl. Mater. Interfaces* 2021, **13**, 36958.

7 (a) C. Törnkvist, J. Bergman and B. Liedberg, *J. Phys. Chem.* 1991, **95**, 3119; (b) S. J. P. Cañete, Z. Zhang, L. Kong, V. L. Schlegel, B. A. Plantz, P. A. Dowben and R. Y. Lai, *Chem. Commun.* 2011, **47**, 11918.